Journal of Geodesy manuscript No.
(will be inserted by the editor)

Continental mass change from GRACE over 2002–2011 and its impact on sea level

O. Baur · M. Kuhn · W.E. Featherstone

Received: date / Accepted: date

O. Baur

Space Research Institute, Austrian Academy of Sciences

8042 Graz, Schmiedlstr. 6, Austria

Phone: +43-316-4120-726, Fax: +43-316-4120-790

E-mail: oliver.baur@oeaw.ac.at

M. Kuhn

Western Australian Centre for Geodesy and The Institute for Geoscience Research,

Curtin University of Technology

Perth, WA 6845, GPO Box U1987, Australia

Phone: +61-8-9266-7603, Fax: +61-8-9266-2703

E-mail: m.kuhn@curtin.edu.au

W.E. Featherstone

Western Australian Centre for Geodesy and The Institute for Geoscience Research,

Curtin University of Technology

Perth, WA 6845, GPO Box U1987, Australia

Phone: +61-8-9266-2734, Fax: +61-8-9266-2703

E-mail: w.featherstone@curtin.edu.au

Abstract Present-day continental mass variation as observed by space gravimetry reveal secular mass decline and accumulation. Whereas the former contribute to sea-level rise, the latter result in sea-level fall. As such, consideration of mass accumulation (rather than focussing solely on mass loss) is important for reliable overall estimates of sea-level change. Using data from the Gravity Recovery And Climate Experiment (GRACE) satellite mission, we quantify mass-change trends in 19 continental areas that exhibit a dominant signal. The integrated mass change within these regions is representative of the variation over the whole land areas. During the integer nine-year period May 2002 to April 2011, GIA-adjusted mass gain and mass loss in these areas contributed, on average, to $-(0.7 \pm 0.4)$ mm/yr of sea-level fall and $+(1.8 \pm 0.2)$ mm/yr of sea-level rise; the net effect was $+(1.1 \pm 0.6)$ mm/yr. Ice melting over Greenland, Iceland, Svalbard, the Canadian Arctic archipelago, Antarctica, Alaska and Patagonia was responsible for $+(1.4 \pm 0.2)$ mm/yr of the total balance. Hence, land-water mass accumulation compensated about 20% of the impact of ice-melt water influx to the oceans. In order to assess the impact of geocentre motion, we converted geocentre coordinates derived from Satellite Laser Ranging (SLR) to degree-one geopotential coefficients. We found geocentre motion to introduce small biases to mass-change and sea-level change estimates; its overall effect is $+(0.1 \pm 0.1)$ mm/yr. This value, however, should be taken with care owing to questionable reliability of secular trends in SLR-derived geocentre coordinates.

Keywords GRACE · Time-variable gravity · Mass variation · Sea level · Geocentre

1 Introduction

Mass transport in the Earth's system is one of the main indicators of contemporary climate change, most notably with regard to sea-level variation estimates and forecasts (e.g., Milne et al., 2009). According to the latest Intergovernmental Panel on Climate Change (IPCC) report (Bindoff et al., 2007), during the period 1993-2003, the total altimetry-observed sea-level change rate of $+(3.1 \pm 0.7)$ mm/yr contained a steric component of $+(1.6 \pm 0.5)$ mm/yr and a land-ice contribution of $+(1.2 \pm 0.4)$ mm/yr.

Cazenave et al. (2009) showed that the overall altimetry-derived sea-level change rate decreased to $+(2.5 \pm 0.4)$ mm/yr during the period 2003-2008. Whereas ocean thermal expansion has reduced since 2003 to $+(0.4 \pm 0.1)$ mm/yr (ibid.), present ice-melt water influx into the oceans is thought to be the main factor driving present sea-level change. Ice sheets have the largest long-term potential effect, where their complete melt would result in a globally averaged sea-level rise of about 70 m (Rahmstorf, 2007), though this varies with position (Farrell and Clark, 1976; Mitrovica et al., 2001; Riva et al., 2010).

Although there is wide consensus on the ongoing secular and periodic changes of the Earth's masses, the quantification of these variations remains somewhat controversial. Satellite gravimetry allows inference of mass variations from time-variable gravity measurements in space. Since 2002, the GRACE (Gravity Recovery And Climate Change Experiment) satellite mission has substantially contributed to an improved understanding of present-day processes. GRACE gravity field time-series have regularly been exploited to derive ice-loss rates within selected regions of interest such as Greenland (e.g., Luthcke et al., 2006), Alaska (e.g., Chen et al., 2006a), Antarctica (e.g., Velicogna and Wahr, 2006a) and Patagonia (e.g., Chen et al., 2007). Land-water

studies typically examine mass-variation characteristics of large river basins and water catchments (e.g., Tapley et al., 2004; Schmidt et al., 2008; Llovel et al., 2010).

This work assesses GRACE-derived continental mass variations on a global scale, including both land-ice and land-water contributions. Our primary objective is to provide some answer to the following question: What can we learn about sea-level change from gravitational signals invoked by land-hydrological mass variations? For this purpose, we investigated continental areas that are most affected by secular mass change as seen by GRACE. As such, this is the first study that selects the regions of interest exclusively on the basis of dominant GRACE signal, rather than by means of *a priori* spatial information. We also shed light on the impact of geocentre motion on these mass trend estimates. Our results are derived from analysis over an integer nine-year period, and hence include an additional one to three years of time-variable gravity fields over previous studies. We compare our results with other findings on land-hydrological changes and estimates of ocean mass trends derived from GRACE.

2 Methods

2.1 Computation of equivalent water height values

Our results are based on monthly gravity field models provided by the Center for Space Research (CSR), University of Texas at Austin. The data is delivered in terms of 4π-normalized spherical harmonic coefficients complete up to degree and order 60. The period of investigation is May 2002 to April 2011, i.e., nine integer years. Data gaps occurred for five months (June 2002, July 2002, June 2003, January 2009, January 2011), thus the total number of 'snapshots' is 103. Residuals of spherical harmonic

coefficients were obtained by subtracting the (assumed static) nine-year means from the monthly values.

We followed one of the "standard" procedures to infer residual (relative to the temporal mean) equivalent water height (ΔEWH) values from GRACE time-variable gravity. This procedure has been reported repeatedly in the literature (e.g., Wahr et al., 1998; Baur et al., 2009); therefore, we give only a very brief outline. The approach approximates vertically integrated mass changes by surface mass densities (Wahr et al., 1998). The numerical constants involved in this formalism are $\rho_{\mathrm{ave}} = 5517\,\mathrm{kg/m^3}$ and $\rho_{\mathrm{w}} = 1000\,\mathrm{kg/m^3}$ for the average mass-density of the solid Earth and of freshwater, respectively; the load Love numbers were taken from Farrell (1972) for the Gutenberg-Bullen model.

As shown by Swenson and Wahr (2006), GRACE-derived spherical harmonic coefficients are contaminated by correlated errors. The errors can be removed by fitting and subtracting a low-order polynomial separately to even and odd coefficients. In order to damp GRACE errors in (de-correlated) high-degree spherical harmonic coefficients, we down-weighted short-scale gravity field features by spatial averaging. Akin to previous studies (cf., Schmidt et al., 2008; Baur et al., 2009; Chen et al., 2009), we used Gaussian smoothing (Jekeli, 1981) with a radius of 500 km.

Prior to analysis, we replaced the CSR $\bar{c}_{20}$ spherical harmonic coefficients by values obtained from Satellite Laser Ranging (SLR) (Cheng and Tapley, 2004). The SLR values of the flattening coefficient have been proven to be more reliable than the GRACE $\bar{c}_{20}$ estimates (e.g., Velicogna and Wahr, 2006b). We used the SLR data provided by the GRACE Tellus Team (`grace.jpl.nasa.gov`), taking both the atmosphere-ocean de-aliasing model (Flechtner, 2007) and the IERS2003 rate for $\bar{c}_{20}$ (McCarthy and Petit, 2004) into account.

2.2 Computation of mass-change rates

In order to avoid aliasing effects of strong seasonal signals and tidal constituents falsifying our trend estimates, we fit ΔEWH time-series with a linear trend function and four sinusoids by least-squares adjustment. The sinusoids account for the annual signal, semi-annual signal and two tidal aliases (Chen et al., 2009), i.e., the S_2 tide (161-day period) and the K_2 tide (3.73-year period). Due to the limited time span of our GRACE gravity field series, our analysis does not account for possible long-term (decadal and longer) periodic changes in hydrology. The standard deviations of the polynomial coefficients were derived from the variance-covariance matrix of the estimated regression parameters (product of the inverse normal equations' matrix with the *a posteriori* variance of unit weight).

Our error bounds are based on error propagation within each individual processing step, starting from the formal errors of the spherical harmonic coefficients as initial error information. However, the consideration of formal errors only has a marginal influence on the derived uncertainties. We suppose that the incorporation of formal errors is only of minor importance, even if they are empirically calibrated in order to more realistically represent the actual noise in GRACE-based monthly solutions (cf. Koch, 2005; Wagner and McAdoo, 2011). The overall error budget is dominated by the adjusted residuals, i.e., the differences between the monthly mass variations and the least-squares fit to these values.

Several recent studies have pointed to potentially accelerated mass-variation processes. Velicogna and Wahr (2006b) found that Greenland ice-mass loss accelerated by about 250% between April 2002 to April 2004 and May 2004 to April 2006. This result was supported by Baur et al. (2012), analyzing various several-year periods and

applying various metric criteria. Rignot et al. (2011) suggested that deglaciation over Greenland and Antarctica accelerated by $+(21.9 \pm 1)\,\mathrm{Gt/yr^2}$ and $+(14.5 \pm 2)\,\mathrm{Gt/yr^2}$, respectively, over the last 18 years. Analyzing GRACE data over the period 2002 to 2009, Velicogna (2009) quantified ice-loss acceleration of $+(30 \pm 11)\,\mathrm{Gt/yr^2}$ in Greenland and $+(26 \pm 14)\,\mathrm{Gt/yr^2}$ in Antarctica.

For most of our regions of interest, statistical hypothesis testing (Student t-test with a 5% level of significance) of the polynomial coefficients revealed that the temporal progress of mass change is better represented by a linear trend function than a second-order polynomial. On the other hand, the difference in mass change over the entire integer nine-year period adopting a linear versus a second-order trend function is negligible. For Greenland, for instance, this difference is far less than 1%, and hence within the error bounds. This discrepancy can be considered as an upper bound, since Greenland is one of the regions most affected by an accelerated mass-variation signature. In this study, we are exclusively interested in change rates over a fixed period. Therefore, we consistently modelled secular mass changes by linear trend functions.

2.3 Correction for signal leakage

Leakage effects cause the GRACE signal to spread out spatially, thus not be concentrated directly over the area of mass variation but also over the surrounding region; theoretically over the whole globe (e.g., Chen et al., 2006b). Therefore, we derived continental mass variations within our selected regions of interest using the leakage correction algorithm developed by Baur et al. (2009).

The procedure isolates and quantifies signal leaking out of each region of interest (leakage-out) and signal leaking into each region of interest (leakage-in). The method is

a combination of extended spatial filters, followed by "calibration" in terms of comparison with forward gravity field modelling. Most notably, the approach is independent of the delineation of the region of interest, provided that it is close to the mass-change location. The total leakage effect is expressed by a single scale factor. We refer the reader to Baur et al. (2009) for a full description of this technique.

2.4 Correction for glacial isostatic adjustment

In order to reduce the impact of glacial isostatic adjustment (GIA) effects from our estimates, we incorporated the GIA model by Paulson et al. (2007). We simply followed the recommendation by the GRACE Tellus Team, referring to it as the temporarily "best" GIA model (`grace.jpl.nasa.gov/data/pgr/`). We assumed the GIA signal to be linear in time, which is justified for the comparatively short period of GRACE data availability (Swenson et al., 2003).

Due to assumptions of ice-load history and mantle viscosity, GIA models are subject to large error bounds. For instance, Wu et al. (2010) estimated the GIA effect over Greenland to be significantly larger compared to previous findings. Riva et al. (2009) showed that the GIA contribution over Antarctica may amount to $+(100 \pm 67)$ Gt/yr in apparent mass gain. In contrast, Velicogna and Wahr (2006a) quantified the change rate to $+(176 \pm 72)$ Gt/yr. Discrepancies in GIA modelling are as yet an unresolved issue, particularly over Antarctica. As such, the choice of the model by Paulson et al. (2007) is somewhat arbitrary; others may apply their preferred GIA corrections.

We assumed an uncertainty level of 30% for the Paulson model. The error bounds of our GIA-corrected mass-change estimates, hence, are subject to the uncertainties of both the regression line slope parameters and GIA model error estimates of 30%.

2.5 Correction for geocentre motion

Satellite gravimetry is insensitive to geocentre motion, defined as the position of the Earth's instantaneous centre of mass (CM) relative to the Earth's centre of figure (CF) (Swenson et al., 2008). In fact, the geocentre undergoes periodic and secular changes. Their omission introduces biases to mass balance estimates (e.g., Chen et al., 2005). Quinn and Ponte (2010) reported that geocentre adjustment over the period July 2003 to June 2007 resulted in approximately +0.2 mm/yr average sea-level change equivalent.

Geocentre motion is directly linked to the degree-1 spherical harmonic coefficients of the gravity field; consequently, the GRACE degree-1 terms are zero by definition. The relation between the 4π-normalized degree-1 coefficients in the CF frame and the geocentre coordinates reads (e.g., Crétaux et al., 2002)

$$c_{10} = \frac{z}{\sqrt{3}a},\ c_{11} = \frac{x}{\sqrt{3}a},\ s_{11} = \frac{y}{\sqrt{3}a}. \tag{1}$$

In Eq. (1), (x, y, z) are the Cartesian coordinates of the instantaneous CM in the CF frame; a indicates the Earth's mean radius.

Several strategies have been proposed to account for geocentre motion. Each relies on external information such as provided by SLR (e.g., Crétaux et al., 2002), GPS (e.g., Blewitt and Clarke, 2003), modeled ocean bottom pressure (e.g., Swenson et al., 2008), or a combination of them (e.g., Wu et al., 2006). Here we used geocentre coordinates of the instantaneous CM relative to the CF derived from SLR (Cheng et al., 2010), cf. Fig. 1; the data is provided by CSR (`ftp.csr.utexas.edu/pub/slr/geocenter/`). We used Eq. (1) to convert geocentre coordinates to degree-1 spherical harmonic coefficients.

Akin to GIA, geocentre motion estimates have large error bounds. According to Fig. 1, the signal-to-noise ratio is less than one for many of the monthly values. Furthermore, in general the reliability of SLR-derived geocentre trends is not yet fully verified. On the other hand, trends in the degree-1 coefficients have a considerable impact on mass-change quantification, especially on regional scales. We thus decided to follow a two-track processing scheme: the first neglects geocentre motion, whereas the second applies corrections according to Fig. 1.

[Fig. 1 about here.]

3 Results

3.1 Regions of interest

Our global assessment of land-hydrological mass changes targets continental areas that exhibit a dominant GRACE signal. We extracted the regions from the ΔEWH pattern evaluated on a regular $1^\circ \times 1^\circ$ grid. Figure 2 (upper panel) presents the mass-variation signals as sensed by GRACE. Prior to region delineation, we corrected the pattern for GIA with the Paulson et al. (2007) model. According to Fig. 2 (lower panel), the Canadian Shield and Antarctica exhibit the strongest GIA signals. Note that after consideration of post-glacial rebound, the signals over Canada and Fennoscandia become small compared to the uncorrected pattern.

[Fig. 2 about here.]

The separation between physically meaningful signals and artifacts caused by GRACE errors is a delicate matter. As a trade-off, we considered only those continental regions that show signal magnitudes stronger than the strongest signal magnitude over the

world's oceans. Hence, the delineation of the regions of interest (RoI) is subject to (positive and negative) trade-off of the signal strength isolines (Fig. 2, lower panel). We found this signal strength isolines to ±75% of the total continental signal magnitude (this value also holds when taking geocentre motion into account). Note that the delineation itself is of secondary importance as different delineations are compensated equally during the leakage-correction procedure (Baur et al., 2009). Hence, the selection criterion only makes a decision on what regions should be considered but the final result is not dependent on spatial extent.

Importantly, the continental signals outside our RoI balance close to zero. In order to quantify the impact of these neglected signals, we compared the balance over the entire land area with the balance within the RoI (only continental area considered). The balances differ by 7%, i.e., neglecting the continental signals outside the RoI potentially introduces an error of 7% to our global budget. Consequently, the total mass variation within our selected RoI is representative of the mass variation over the whole continents. As far as the correction for geocenter motion is concerned, the balance over the entire land area and the balance within the RoI differ by about 10%. This additional error is uncritical owing to the comparatively small magnitude of the mass-variation signal caused by geocenter motion.

Our trade-off criterion implies the signal over the oceans to be the upper bound of signals caused by GRACE errors. Certainly, this trade-off criterion is somewhat arbitrary. Nevertheless, the choice is reasonable for two reasons. Firstly, most of our RoI have been reported earlier to show secular mass variation. Secondly, our integrated regional mass budget is representative for the global mass budget (with a potential error of 7%, as highlighted before).

We found 19 RoI to be affected by contemporary secular mass change (Fig. 2, lower panel). Most of these regions can be attributed to either glaciated areas (Greenland, Antarctica, Alaska, Patagonia), large river catchment systems (Amazon, Parana, Zambezi/Okavango, Brahmaputra/Ganges, Volga, Euphrates/Tigris, Niger, Godavari/Krishna) or residual GIA (Canada, Fennoscandia). For the time being, we omit classification of the signals in Central Siberia, Kamchatka and Australia. These signals are amongst the weakest, and hence could be artifacts that are misinterpreted as meaningful signals.

3.2 Mass-change trends

Table 1 summarizes our findings of mass-change trends. The magnitudes range from a few Gt/yr up to more than 300 Gt/yr. Note that the region "Greenland" includes Iceland, Svalbard, and the Canadian Arctic archipelago. The error bounds listed in Table 1 were obtained by quadratic summation of the GRACE errors, the GIA errors, and the errors from geocentre motion. Due to GIA uncertainties, the error bounds for regions with a strong postglacial rebound signal are particularly large. This turns out most clearly for Canada, as the Canadian Shield exhibits the strongest GIA signal (Fig. 2).

As a general statement, geocentre motion correction implies mass loss in the Northern Hemisphere and mass gain in the Southern Hemisphere. This is subject to the dominant (negative) trend of the z-component of geocentre motion compared to the x-y component (Métivier et al., 2010), cf. Fig. 1. As a consequence, RoI in polar areas are affected most by geocentre motion corrections.

[Table 1 about here.]

3.3 Sea-level change equivalent

Mass gain or loss over land areas can be translated into homogeneous water changes over the world's oceans (Table 1, last two columns). Consequently, each region of interest according to Fig. 2 either contributes to sea-level rise (caused by continental mass loss) or sea-level fall (caused by continental mass gain). In order to convert our regional mass-variation budgets to a global budget, we simply summed up the individual contributions (Table 1, last three rows). The error bounds were determined by quadratic summation of the overall GRACE error (quadratic summation of individual components), the overall GIA error (arithmetic summation of individual components), and the overall geocentre motion error (quadratic summation of individual components).

If geocentre motion is neglected, mass variations in the RoI caused $+(1.8\pm0.2)$ mm/yr in sea-level rise and $-(0.7 \pm 0.4)$ mm/yr in sea-level fall; the overall balance is $+(1.1 \pm 0.6)$ mm/yr. The large error bound for the overall estimate stems from the sea-level fall contributions being more subject to GIA errors. The contribution from glaciated areas (Greenland, Antarctica, Alaska and Patagonia) is $+(1.4 \pm 0.2)$ mm/yr. This rate does not include the signal in northern India, which might partially be caused by the retreat of Himalayan glaciers (Matsuo and Heki, 2010) and partially by groundwater depletion (Tiwari et al., 2009). Due to the limited spatial resolution of GRACE data, the separation of these two sources remains a yet unsolved issue (Cazenave and Chen, 2010). Land-water variation corresponds to a sea level change equivalent of $-(0.2 \pm 0.3)$ mm/yr. Geocentre motion affects our sea-level rise and fall estimates equally. The net effect is $+(0.1 \pm 0.1)$ mm/yr.

4 Discussion and conclusions

Our global assessment of continental mass changes isolates 19 regions that are significantly affected by mass loss or mass gain. Almost all of them can be attributed to glaciologically or hydrologically active areas such as ice sheets or river basins. Some of the regions are characterized by rather weak GRACE signals, and hence may be artefacts misinterpreted as mass change. Regardless, the mass-change magnitudes of these candidates are comparatively small, i.e., their exclusion has only minor influence on our results and the conclusions reached.

Our selection criterion was according to dominant GRACE signal. This strategy is in contrast to previous GRACE studies. For instance, Llovel et al. (2010) defined 33 river basins for their global land water storage investigation. Jacob et al. (2012) quantified mass variation in 20 glaciated areas to shed light on recent deglaciation-driven sea-level rise. The benefit of our approach is that we avoided any *a priori* spatial information. Moreover, this study includes both land-ice and land-water contributions. As such, our investigation is more akin to the work by Riva et al. (2010). They quantified the global budget by taking the GRACE signal over the entire land area into account.

Table 2 provides an overview on the results obtained from the different investigations. Although the studies refer to inconsistent periods, they are in general agreement. Note that the land-ice contribution derived by Jacob et al. (2012) is dominated by mass variation over Greenland (including Iceland, Svalbard, Canadian Arctic archipelago), Antarctica, Alaska and Patagonia. From a comparison with the results by Riva et al. (2010), we again conclude that the integrated mass change within our selected RoI is representative for the variation over the whole continents.

[Table 2 about here.]

A closer look to the RoI reveals that on the level of individual catchments significant trend estimate discrepancies exist. These discrepancies are mainly due to the differing periods (cf. Baur, 2012). As an example, Llovel et al. (2010) quantified mass variation in the Amazon basin to $+(78 \pm 9)$ Gt/yr; our estimate is $+(43 \pm 14)$ Gt/yr. The re-evaluation over the period August 2002 to July 2009 yields our balance to become $+(71 \pm 19)$ Gt/yr, which is in line with the change rate found by Llovel et al. (2010). The same conclusion holds for the Zambesi/Okavango basin with values of $+(21 \pm 3)$ Gt/yr and $+(27 \pm 12)$ Gt/yr obtained by Llovel et al. (2010) and our re-computation, respectively. Further comparisons are not possible as the basin delineations used by Llovel et al. (2010) significantly differ from that one we used. Jacob et al. (2012) estimated mass change over Greenland (including Iceland, Svalbard, Canadian Arctic archipelago), Antarctica, Alaska and Patagonia to $-(300 \pm 12)$ Gt/yr, $-(165 \pm 72)$ Gt/yr, $-(46 \pm 7)$ Gt/yr, and $-(23 \pm 9)$ Gt/yr, respectively; our (geocentre-corrected) change rates are $-(323 \pm 26)$ Gt/yr, $-(104 \pm 48)$ Gt/yr, $-(56 \pm 7)$ Gt/yr, and $-(10 \pm 3)$ Gt/yr.

We used SLR information to capture the impact of CM-to-CF differences on mass trends and sea-level change. In terms of equivalent sea-level change, we quantified geocentre motion to introduce a bias of $+(0.1 \pm 0.1)$ mm/yr to our analysis. This value is in broad agreement with the findings by Quinn and Ponte (2010), who reported that geocentre variations over the period July 2003 to June 2007 resulted in approximately $+0.2$ mm/yr average sea-level change equivalent. Nonetheless, we emphasize that for the time being the translation of trends in geocentre coordinates to mass change remains critical. The adoption of additional geocentre time series (e.g., Rietbroek et al., 2011) could improve the knowledge about uncertainties in geocentre correction.

Our estimated non-steric ocean mass trends of $+(1.1 \pm 0.6)$ mm/yr (geocentre-neglected) and $+(1.2 \pm 0.6)$ mm/yr (geocentre-corrected) include both land-ice and land-water contributions. As pointed out earlier, the neglect of continental signals outside our selected RoI potentially introduces an error of 7% in our global budget, corresponding to an additional trend of +0.1 mm/yr. Our change rates hold for the period May 2002 to April 2011, i.e., nine integer years. Analyzing gravity field solutions from 2002 to 2006 over oceanic areas, Lombard et al. (2007) estimated the trend of the ocean mass change to be $+(1.2 \pm 0.5)$ mm/yr. Willis et al. (2008) and Leuliette and Miller (2009) found the GRACE-derived ocean mass trend to be $+(0.8 \pm 0.8)$ mm/yr and $+(0.8 \pm 0.5)$ mm/yr, respectively. Leuliette and Willis (2011) quantified the rate as $+(1.1 \pm 0.6)$ mm/yr for the period January 2005 to September 2010. Noteworthy, these results are in good agreement, although they are based on different (and sometimes non-integer-year) time periods, and hence prone to inter-annual variability erroneously interpreted as part of the mass-change trend.

The sum of ocean mass trend and steric sea-level change provides an estimate for the total sea-level variation. Based on Argo profiles, the steric component has been quantified to $+(0.4 \pm 0.1)$ mm/yr and $+(0.8 \pm 0.8)$ mm/yr by Cazenave et al. (2009) and Leuliette and Miller (2009), respectively. These numbers differ considerably. Furthermore, it should be noted that the Argo-observed steric component only accounts for seawater density changes in the upper oceanic layer down to depths of about 1000 m. As reported by Antonov et al. (2005), deep steric changes are considerably smaller. On the other hand, Song and Colberg (2011) found that ocean warming below 700 m might have contributed +1.1 mm/yr to sea level rise. In summary, at present steric sea-level change computation is subject to large uncertainty. In order to provide some numbers regarding the total sea-level change, adding the steric com-

ponent of $+(0.5 \pm 0.5)$ mm/yr (Leuliette and Willis, 2011) to our non-steric ocean mass trends yields $+(1.6 \pm 0.8)$ mm/yr (geocentre-neglected) and $+(1.7 \pm 0.8)$ mm/yr (geocentre-corrected).

For the time being, it remains an open issue whether the global assessment of GRACE-derived secular continental mass variations closes the overall sea-level change budget. For instance, during the period 2003–2008, Cazenave et al. (2009) quantified the altimetry-observed trend in sea-level as $+(2.5 \pm 0.4)$ mm/yr. Within a similar time span, Leuliette and Miller (2009) obtained an altimetry-based trend of $+(2.4 \pm 1.1)$ mm/yr. Owing to the large uncertainties of the involved individual contributions, the sum of the steric and non-steric sea-level variation fits to the findings from altimetry, and hence provides a solution to the sea-level enigma (Munk, 2002).

Acknowledgements The data used in this study were made freely available by the Center for Space Research. This work was partly supported under the Australian Research Council's Discovery Projects funding scheme (project number DP0877381). Michael Kuhn acknowledges the support of a Curtin Research and Teaching Fellowship. The views expressed herein are those of the authors and are not necessarily those of the Australian Research Council. We kindly acknowledge helpful comments by four anonymous reviewers and the editor of the manuscript.

References

Antonov JI, Levitus S, Boyer TP (2005) Thermosteric sea level rise. 19552003, Geophys Res Lett 32, L12602. doi: 10.1029/2005GL023112

Baur O, Kuhn M, Featherstone WE (2009) GRACE-derived ice-mass variations over Greenland by accounting for leakage effects. J Geophys Res 114, B06407. doi: 10.1029/2008JB006239

Baur O (2012) On the computation of mass-change trends from GRACE gravity field time-series. J Geodyn, in press. doi: 10.1016/j.jog.2012.03.007

Baur O, Kuhn M, Featherstone WE (2012) GRACE-derived linear and non-linear secular mass variations over Greenland. In: Sneeuw N, Novák P, Crespi M, Sansò F (Eds) VII Hotine-Marussi Symposium on Mathematical Geodesy, IAG Series 137, Springer Berlin Heidelberg, 381–386

Bindoff NL, et al. (2007) Observations: Oceanic climate change and sea level. In: Solomon S, et al. (Eds) IPCC Climate Change 2007: The Physical Science Basis, 385–432, Cambridge University Press

Blewitt G, Clarke P (2003) Inversion of Earth's changing shape to weigh sea level in static equilibrium with surface mass redistribution. J Geophys Res 108, 2311. doi: 10.1029/2002JB002290

Cazenave A, Dominh K, Guinehut S, Berthier E, Llovel W, Ramillien G, Ablain M, Larnicol G (2009) Sea level budget over 2003–2008: A reevaluation from GRACE space gravimetry, satellite altimetry and Argo. Glob Planet Change 65: 83–88. doi: 10.1016/j.gloplacha.2008.10.004

Cazenave A, Chen J (2010) Time-variable gravity from space and present-day mass redistribution in the Earth system. Earth Planet Sci Lett 298: 263–274. doi: 10.1016/j.epsl.2010.07.035

Chen JL, Rodell M, Wilson CR, Famiglietti JS (2005) Low degree spherical harmonic influences on Gravity Recovery and Climate Experiment (GRACE) water storage estimates. Geophys Res Lett 32, L14405. doi: 10.1029/2005GL022964

Chen JL, Tapley BD, Wilson CR (2006a) Alaskan mountain glacial melting observed by satellite gravimetry. Earth Planet Sci Lett 248: 368–378. doi: 10.1016/j.epsl.2006.05.039

Chen JL, Wilson CR, Blankenship DD, Tapley BD (2006b) Antarctic mass rates from GRACE. Geophys Res Lett 33, L11502. doi: 10.1029/2006GL026369

Chen JL, Wilson CR, Tapley BD, Blankenship DD, Ivins ER (2007) Patagonia Icefield melting observed by Gravity Recovery and Climate Experiment (GRACE). Geophys Res Lett 34, L22501. doi: 10.1029/2007GL031871

Chen JL, Wilson CR, Seo K-W (2009) S_2 tide aliasing in GRACE time-variable gravity solutions. J Geod 83: 679–687. doi: 10.1007/s00190-008-0282-1

Cheng M, Tapley BD (2004) Variations in the Earth's oblateness during the past 28 years. J Geophys Res 109, B09402. doi: 10.1029/2004JB003028

Cheng MK, Tapley BD, Ries JC (2010) Geocenter variations from analysis of SLR data. IAG Commission 1 Symposium 2010, Reference Frames for Applications in Geosciences (REFAG2010), Marne-La-Vallee, France, 4–8 October 2010

Crétaux J-F, Soudarin L, Davidson FJM, Gennero M-C, Bergé-Nguyen M, Cazenave A (2002) Seasonal and interannual geocentre motion from SLR and DORIS measurements: Comparison with surface loading data. J Geophys Res 107, 2374. doi: 10.1029/2002JB001820

Farrell WE (1972) Deformation of the Earth by surface loading. Rev Geophys 10: 761–797

Farrell WE, Clark JA (1976) On postglacial sea level. Geophys J R Astr Soc 46: 647–667

Flechtner F (2007) AOD1B product description document for product releases 01 to 04. Rev 3.1

Jacob T, Wahr J, Pfeffer WT, Swenson S (2012) Recent contributions of glaciers and ice caps to sea level rise. Nature, accepted. doi: 10.1038/nature10847

Jekeli C (1981) Alternative methods to smooth the Earth's gravity field. Rep 327, Dep of Geod Sci and Surv, Ohio State Univ, Columbus

Koch, KR (2005) Determining the maximum degree of harmonic coefficients in geopotential models by Monte Carlo methods. Stud Geophys Geod 49: 259–275. doi: 10.1007/s11200-005-0009-1

Leuliette EW, Miller L (2009) Closing the sea level rise budget with altimetry, Argo, and GRACE. Geophys Res Lett 36, L04608. doi: 10.1029/2008GL036010

Leuliette EW, Willis JK (2011) Balancing the sea level budget. Oceanography 24: 122–129. doi: 10.5670/oceanog.2011.32

Llovel W, Becker M, Cazenave A, Crétaux J-F, Ramillien G (2010) Global land water storage change from GRACE over 2002–2009; Inference on sea level. C R Geoscience 342: 179–188. doi: 10.1016/j.crte.2009.12.004

Lombard A, Garcia D, Ramillien G, Cazenave A, Biancale R, Lemoine JM, Flechtner F, Schmidt R, Ishii M (2007) Estimation of steric sea level variations from combined GRACE and Jason-1 data. Earth Planet Sci Lett 254: 194–202. doi: 10.1016/j.epsl.2006.11.035

Luthcke SB, Zwally HJ, Abdalati W, Rowlands DD, Ray RD, Nerem RS, Lemoine FG, McCarthy JJ, Chinn DS (2006) Recent Greenland ice mass loss by drainage system from satellite gravity observations. Science 314: 1286–1289. doi: 10.1126/science.1130776

Matsuo K, Heki K (2010) Time-variable ice loss in Asian high mountains from satellite gravimetry. Earth Planet Sci Lett 290: 30–36. doi: 10.1016/j.epsl.2009.11.053

McCarthy DD, Petit G (2004) IERS Conventions (2003). IERS Technical Note 32

Métivier L, Greff-Lefftz M, Altamimi Z (2010) On secular geocentre motion: The impact of climate changes. Earth Planet Sci Lett 296: 360–366.

doi: 10.1016/j.epsl.2010.05.021

Milne GA, Gehrels WR, Hughes CW, Tamisiea ME (2009) Identifying the causes of sea-level change. Nature Geosci 2: 471–478. doi: 10.1038/ngeo544

Mitrovica JX, Tamisiea ME, Davis JL, Milne GA (2001) Recent mass balance of polar ice sheets inferred from patterns of global sea-level change. Nature 409: 1026–1029. doi: 10.1038/35059054

Munk W (2002) Twentieth century sea level: an enigma. Proc Natl Acad Sci USA 99: 6550–6555

Quinn KJ, Ponte RM (2010) Uncertainty in ocean mass trends from GRACE. Geophys J Int 181: 762–768. doi: 10.1111/j.1365-246X.2010.04508.x

Paulson A, Zhong S, Wahr J (2007) Inference of mantle viscosity from GRACE and relative sea level data. Geophys J Int 171: 497–508. doi: 10.1111/j.1365-246X.2007.03556.x

Rahmstorf S (2007) A semi-empirical approach to projecting future sea-level rise. Science 315: 368–370. doi: 10.1126/science.1135456

Rietbroek R, Fritsche M, Brunnabend S-E, Daras I, Kusche J, Schröter J, Flechtner F, Dietrich R (2011) Global surface mass from a new combination of GRACE, modelled OBP and reprocessed GPS data. J Geodyn, in press. doi: 10.1016/j.jog.2011.02.003

Rignot E, Velicogna I, van den Broeke M, Monaghan A, Lenaerts J (2011) Acceleration of the contribution of the Greenland and Antarctic ice sheets to sea level rise. Geophys Res Lett 38, L05503. doi: 10.1029/2011GL046583

Riva REM, Gunter BC, Urban TJ, Vermeersen BLA, Lindenbergh RC, Helsen MM, Bamber JL, van de Wal RSW, van den Broeke MR, Schutz BE (2009) Glacial Isostatic Adjustment over Antarctica from combined ICESat and GRACE satellite data. Earth Planet Sci Lett 288: 516–523. doi: 10.1016/j.epsl.2009.10.013

Riva REM, Bamber JL, Lavallée DA, Wouters B (2010) Sea-level fingerprint of continental water and ice mass change from GRACE. Geophys Res Lett 37, L19605. doi: 10.1029/2010GL044770

Schmidt R, Petrovic S, Güntner A, Barthelmes F, Wünsch J, Kusche J (2008) Periodic components of water storage changes from GRACE and global hydrology models. J Geophys Res 113, B08419. doi: 10.1029/2007JB005363

Song YT, Colberg F (2011) Deep ocean warming assessed from altimeters, Gravity Recovery and Climate Experiment, in situ measurements, and a nonBoussinesq ocean general circulation model. J Geophys Res 116, C02020. doi: 10.1029/2010JC006601

Swenson S, Wahr J, Milly PCD (2003) Estimated accuracies of regional water storage variations inferred from the Gravity Recovery and Climate Experiment (GRACE). Water Resour Res 39, 1223. doi: 10.1029/2002WR001808

Swenson S, Wahr J (2006) Post-processing removal of correlated errors in GRACE data. Geophys Res Lett 33, L08402. doi: 10.1029/2005GL025285

Swenson S, Chambers D, Wahr J (2008) Estimating geocentre variations from a combination of GRACE and ocean model output. J Geophys Res 113, B08410. doi: 10.1029/2007JB005338

Tapley BD, Bettadpur S, Watkins M, Reigber C (2004) The Gravity Recovery and Climate Experiment: mission overview and early results. Geophys Res Lett 31, L09607. doi: 10.1029/2004GL019920

Tiwari VM, Wahr J, Swenson S (2009) Dwindling groundwater resources in northern India, from satellite gravity observations. Geophys Res Lett 36, L18401. doi: 10.1029/2009GL039401

Velicogna I, Wahr J (2006a) Measurements of time-variable gravity show mass loss in Antarctica. Science 311: 1754–1756. doi: 10.1126/science.1123785

Velicogna I, Wahr J (2006b) Acceleration of Greenland ice mass loss in spring 2004. Nature 443: 329–331. doi: 10.1038/nature05168

Velicogna I (2009) Increasing rates of ice mass loss from the Greenland and Antarctic ice sheets revealed by GRACE. Geophys Res Lett 36, L19503. doi: 10.1029/2009GL040222

Wagner CA, McAdoo DC (2011) Error calibration of geopotential harmonics in recent and past gravitational fields. J Geod: online first. doi: 10.1007/s00190-011-0494-7

Wahr J, Molenaar M, Bryan F (1998) Time variability of the Earth's gravity field: Hydrological and oceanic effects and their possible detection using GRACE. J Geophys Res 103: 30,205–30,229. doi: 10.1029/98JB02844

Willis JK, Chambers DP, Nerem RS (2008) Assessing the globally averaged sea level budget on seasonal to interannual timescales. J Geophys Res 113, C06015. doi: 10.1029/2007JC004517

Wu X, Heflin MB, Ivins ER, Fukumori I (2006) Seasonal and interannual global surface mass variations from multisatellite geodetic data. J Geophys Res 111, B09401. doi: 10.1029/2005JB004100

Wu X, Heflin MB, Schotman H, Vermeersen BLA, Dong D, Gross RS, Ivins ER, Moore AW, Owen SE (2010) Simultaneous estimation of global present-day water transport and glacial isostatic adjustment. Nature Geosci 3: 642–646. doi: 10.1038/ngeo938

List of Figures

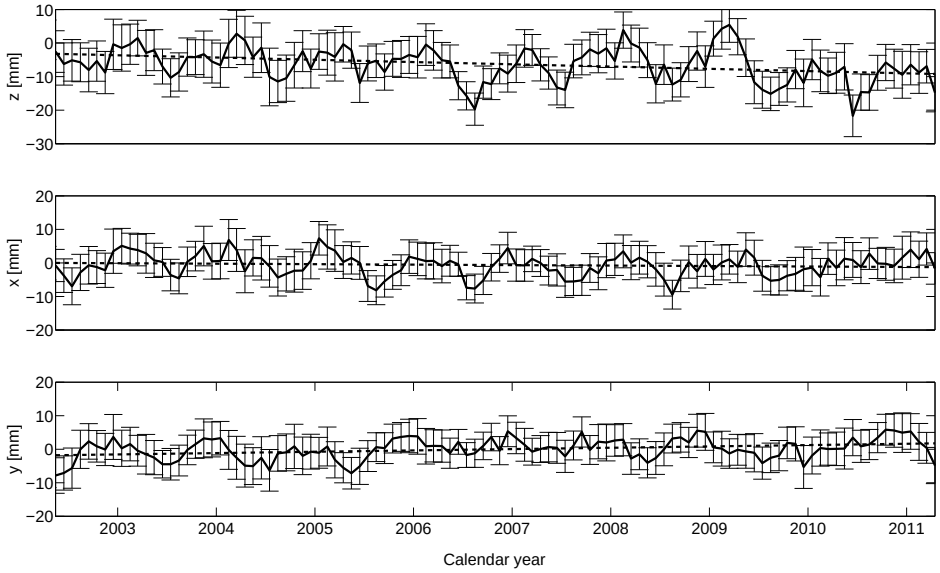

Fig. 1 SLR-derived geocentre motion from May 2002 to April 2011. Solid lines: Cartesian coordinates of the instantaneous CM in the CF frame; dashed lines: linear trend functions. The error bars represent the standard deviation of the monthly values.

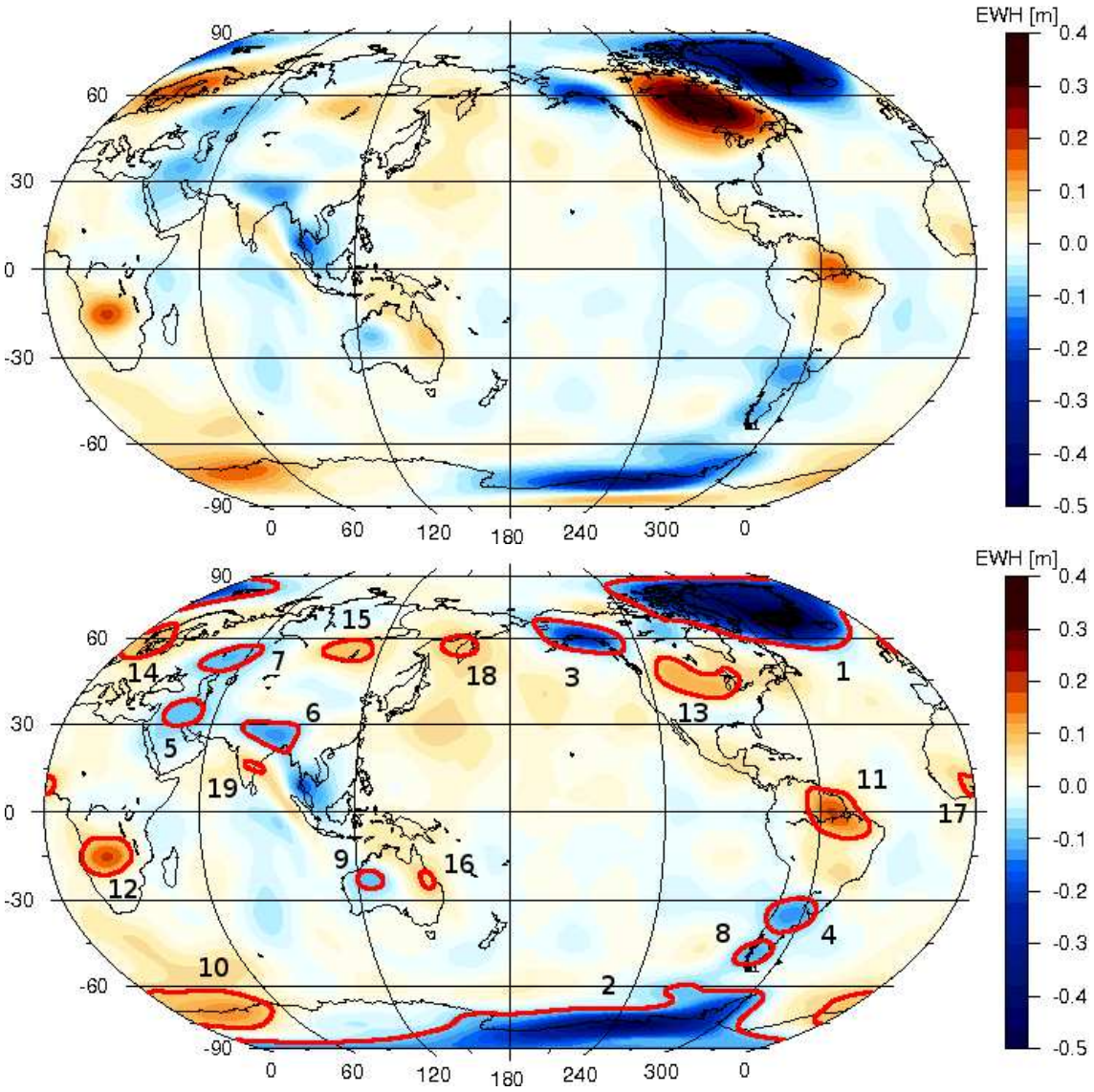

Fig. 2 Secular trends in terms of equivalent water height from May 2002 to April 2011. A regression line was fitted to time-series of residual EWH values at each point of a global $1^\circ \times 1^\circ$ grid. Upper panel: no corrections for GIA (and geocentre motion) applied. Lower panel: corrections for GIA applied. Delineated areas indicate regions of interest considered in this study; their choice is according to a trade-off between physically meaningful signals and potential artifacts caused by GRACE errors. Numbers correspond to regions shown in Table 1.

List of Tables

Table 1 Mass-change trend and average sea-level change equivalent for the regions of interest as shown in Fig. 2.

Region		Mas-change trend (Gt/yr)		Sea-level change equivalent (mm/yr)	
		geocentre-neglected	geocentre-corrected	geocentre-neglected	geocentre-corrected
1	Greenland [a]	-286 ± 15	-323 ± 26	0.79 ± 0.04	0.89 ± 0.07
2	West Antarctica	-201 ± 40	-169 ± 46	0.56 ± 0.11	0.47 ± 0.13
3	Alaska	-47 ± 5	-56 ± 7	0.13 ± 0.01	0.16 ± 0.02
4	Parana	-27 ± 6	-26 ± 7	0.07 ± 0.02	0.07 ± 0.02
5	Euphrates/Tigris	-25 ± 5	-27 ± 6	0.07 ± 0.01	0.08 ± 0.02
6	Brahmaputra/Ganges	-24 ± 4	-25 ± 6	0.07 ± 0.01	0.07 ± 0.02
7	Volga	-24 ± 5	-28 ± 6	0.07 ± 0.01	0.08 ± 0.02
8	Patagonia	-12 ± 2	-10 ± 3	0.03 ± 0.01	0.03 ± 0.01
9	West Australia	-9 ± 2	-7 ± 3	0.03 ± 0.01	0.02 ± 0.01
10	East Antarctica	51 ± 10	65 ± 13	-0.14 ± 0.03	-0.18 ± 0.04
11	Amazon	50 ± 13	43 ± 14	-0.14 ± 0.04	-0.12 ± 0.04
12	Zambezi/Okavango	38 ± 7	40 ± 8	-0.10 ± 0.02	-0.11 ± 0.02
13	Canada	51 ± 110	25 ± 111	-0.14 ± 0.31	-0.07 ± 0.31
14	Fennoscandia	18 ± 23	12 ± 23	-0.05 ± 0.06	-0.03 ± 0.06
15	Central Siberia	13 ± 2	10 ± 4	-0.04 ± 0.01	-0.03 ± 0.01
16	East Australia	12 ± 3	14 ± 3	-0.03 ± 0.01	-0.04 ± 0.01
17	Niger	9 ± 2	8 ± 2	-0.03 ± 0.01	-0.02 ± 0.01
18	Kamchatka	9 ± 2	6 ± 3	-0.02 ± 0.01	-0.02 ± 0.01
19	Godavari/Krishna	3 ± 1	4 ± 1	-0.01 ± 0.00	-0.01 ± 0.00
Cumulative sea-level rise				1.8 ± 0.2	1.9 ± 0.2
Cumulative sea-level fall				-0.7 ± 0.4	-0.6 ± 0.4
Balance				1.1 ± 0.6	1.2 ± 0.6

[a] Including Iceland, Svalbard, and the Canadian Arctic archipelago.
Uncertainties are given at the 95% (2σ) confidence level.

Table 2 Contributions of continental mass variation to average sea-level change (mm/yr).

Study	Period	Land-ice	Land-water	Total
Llovel et al. (2010)	August 2002–July 2009	-	$-(0.2 \pm 0.1)$	-
Jacob et al. (2012)	January 2003–December 2010	$+(1.5 \pm 0.3)$	-	-
Riva et al. (2010)	February 2003–February 2009	$+(1.0 \pm 0.2)$ [a]	$-(0.1 \pm 0.3)$	$+(1.0 \pm 0.4)$
This study (geocentre-corrected)	May 2002–April 2011	$+(1.4 \pm 0.2)$ [a]	$-(0.1 \pm 0.3)$	$+(1.2 \pm 0.6)$

[a] Greenland (incl. Iceland, Svalbard, Canadian Arctic archipelago), Antarctica, Alaska and Patagonia